Lab on a Chip

Cite this: *Lab Chip*, 2011, **11**, 1132

www.rsc.org/loc

PAPER

Controlling the contents of microdroplets by exploiting the permeability of PDMS†

Jung-uk Shim,‡[ab] Santoshkumar N. Patil,‡[a] James T. Hodgkinson,[ab] Steven D. Bowden,[b] David R. Spring,[a] Martin Welch,[b] Wilhelm T.S. Huck,*[ac] Florian Hollfelder*[b] and Chris Abell*[a]

Received 19th November 2010, Accepted 20th January 2011
DOI: 10.1039/c0lc00615g

A microfluidic device capable of exploiting the permeability of small molecules through polydimethylsiloxane (PDMS) has been fabricated in order to control the contents of microdroplets stored in storage wells. We demonstrate that protein precipitation and crystallization can be triggered by delivery of ethanol from a reservoir channel, thus controlling the protein solubility in microdroplets. Likewise quorum sensing in bacteria was triggered by delivery of the auto-inducer *N*-(3-oxododecanoyl)-L-homoserine lactone (OdDHL) through the PDMS membrane of the device.

Introduction

Microdroplets in microfluidics are now established as a format for carrying out chemical and biological experiments at the pico- to nanolitre scale.[1–5] An individual water-in-oil droplet compartment serves as the equivalent of the conventional test tube. Droplets can be rapidly produced, processed and interrogated for high-throughput experiments while they are moving through microchannels.[6] Alternatively, interrogation of droplet arrays in which droplets are held static gives high quality data, allowing even single cell or single molecule measurements.[7–10] The droplet boundary can be set-up to prevent transfer processes (*e.g.* by diffusion) and cross-contamination can be minimized through the judicious choice of surfactant, its concentration and other added components[11–13] or by using fluorinated surfactant/oil systems.[8,14–16]

Several formats for the addition of reagents to initiate or terminate a process have been developed. Individual droplets in a moving droplet stream can be merged or reagent added *e.g.* by electrocoalescence,[17–20] destabilization of the droplet interface by surfactant,[21–23] or by channel surface patterning.[24]

The delivery of reagents to static droplet arrays presents different challenges. It has been shown that static droplets can be fused by electrocoalescence[18,25] or by a laser-induced thermocapillary force.[26,27] However, these methods require side-by-side positioning of droplets and the degrees of freedom over the amount of reagent to be delivered are limited by the proximity of neighboring droplets.

The work described in this paper demonstrates the ability to manipulate the contents of droplets based on the permeability of the PDMS of the device. The compatibility of PDMS with organic solvents has previously been studied by comparing the swelling ratio of PDMS in various solvents and their solubilities.[28] The ability of hydrophobic small molecules (exemplified by Nile red and quinine) to permeate PDMS has been described.[29] For example, the permeability of PDMS has been exploited in the removal of trace organic compounds from an aqueous sample.[30,31] There have also been attempts to reduce the permeability of PDMS to small molecules by pre-adsorbing bovine serum albumin (BSA) to the surface,[32] by coating the PDMS with silane[33] and by using a large excess of cross-linking reagents.[34] In addition, the adsorption of a hormone onto PDMS was studied in a microfluidic device.[35] We now address the potential of the permeability of PDMS for initiating multiple processes in droplets.

In order to utilize the diffusion of small molecules through PDMS to microdroplets trapped in resting positions, a microfluidic device was built by multilayer soft lithography.[36] This device contained fluid supply channels (reservoir channel) below the droplets (Fig. S1, ESI†)[9,37] from which small molecules can be supplied for diffusion across the PDMS membrane, and eventually transported into the trapped droplets.

In this work two processes that are influenced by small molecule *stimuli* were probed, namely protein crystallization and the control of bacterial gene expression by quorum sensing molecules. Both processes have been previously addressed in microdroplets.[23,37–41] We now report that ethanol and quorum sensing molecules can be supplied into droplets in a controlled

[a]*Department of Chemistry, University of Cambridge, Cambridge, UK. E-mail: ca26@cam.ac.uk*
[b]*Department of Biochemistry, University of Cambridge, Cambridge, UK. E-mail: fh111@cam.ac.uk*
[c]*Radboud University Nijmegen, Institute for Molecules and Materials, 6525 AJ Nijmegen, The Netherlands. E-mail: w.huck@science.ru.nl; Tel: +44 1223 336405*

† Electronic supplementary information (ESI) available: A detailed image of the microfluidic device, a graph of the solubility and log *P*, resulting images of control experiments, GFP expressions measured in a plate reader, and a movie showing the process of protein crystallization. See DOI: 10.1039/c0lc00615g

‡ These authors contributed equally to this work.

fashion *via* the permeable PDMS membrane from the reservoir channel. Delivery of ethanol is shown to trigger protein precipitation and crystallization by addition of a co-solvent that lowers the protein solubility, thus creating a supersaturated solution and increasing the crystallization propensity. Delivery of a small molecule (an auto-inducer of quorum sensing) triggers a cellular response that is measured indirectly by expression of a reporter gene encoding a fluorescent protein.

Materials and methods

Device design

The device contains an array of 2000 wells in the storage area (Fig. S1, ESI†). The droplet deposition is controlled by inlet valves and occurs *via* the channels shown in Fig. S1a†. Small molecules are administered after the wells have been filled with droplets *via* a reservoir channel that is separated from the wells by a thin PDMS membrane (15 μm, Fig. S1b†). Droplets were stable over 12 hours as assessed by visual inspection.[9] No fusion or break-up of droplets was observed as a result of the addition of solutes in the reservoir channels.

Device fabrication

The device was drawn with AutoCad (AutoDesk) and photolithographic masks were fabricated on transparent plastics (Circuit Graphics, Essex, UK). A positive photoresist (AZ-9260, AZ Electronic Material) was used to build the valve channels[42] and negative photoresists (SU8-2025, SU8-2007 Microchem Inc.) were employed to fabricate the flow channel, wells and valve-reservoir channel. A commercially available PDMS kit (Sylgard 184, Dow Corning) composed of a pre-polymer and a cross-linker was used in the recommended weight ratio of 10 : 1. Two masters were required to fabricate the double-layered microfluidic device.[37] Mixed, degassed liquid PDMS was poured onto the first master and cured at 75 °C for 25 minutes. The resulting flexible silicone rubber was removed, leaving relief features from the master imprinted onto the PDMS slab. Injection holes were punched through the PDMS with lure stub adapters to insert tubings that deliver the fluid into the device. In order to fabricate the control channel and the reservoir in the device, a thin PDMS layer was manufactured onto the face of the PDMS slab covering them with a glass substrate. This thin layer was formed by spinning liquid PDMS onto the second master. The wafer was cured at 85 °C for 5 minutes. After alignment and assembly of the first PDMS slab on the second master, the device was heated again at 85 °C for 30 minutes to enhance adhesion between two PDMS layers.[43] Injection holes were punched to insert tubing. The resulting PDMS slab was sealed against a glass slide after plasma treatment.[44] CYTOP (Asahi Glass company) was coated on the flow channels to prevent the water sticking onto the PDMS walls.

Device operation

Aqueous droplets were formed in fluorinated oil (FC-40, Fluorinert™) previously mixed with surfactants (2% w/w; EA-surfactant, Raindance Technologies) to prevent the coalescence of droplets.[14] The reservoir constructed underneath the wells supplied small molecules and organic solvents to droplets through the PDMS membrane. At the same time the reservoir maintained the volume of stored droplets from water evaporation of microdroplets. Gene expression in cells was induced at a constant temperature of 30 °C.

Optical detection

Fluorescence images were taken on an inverted microscope (IX71, Olympus) using a colliminated LED light source (M455L2-C1, Thorlab) for widefield illumination operated in epifluorescence mode. In order to monitor large numbers of arrayed droplets, the device was mounted on a computer-controlled motorized stage (H117 ProScan II, Prior Scientific) that moved the device in a pre-determined pattern. To minimize photobleaching of green fluorescent protein (GFP) produced in cells, droplets were illuminated only during the acquisition by means of a computer-controlled LED illumination unit (M455L2-C1, Thorlab) using the same objective (UPLSAPO 40X2, Olympus). An EMCCD camera (Xion^{+}, Andor Technologies) was used to acquire images, which were saved to the computer for offline analysis. Automatic acquisitions and image analysis were performed using softwares written in LabView (National Instruments). The fluorescence of GFP was measured from the integration of all green *foci* above the droplet background.

Materials

Chemicals were obtained from Sigma-Aldrich unless otherwise noted.

Protein crystallization

The initial concentration of protein was 59.4 mg ml^{-1} dissolved in 0.2 M sodium chloride, 0.05 M sodium acetate (pH 4.5).

Cell preparation

Escherichia coli (*E. coli*) cells (DH5α) harboring a pMHLAS plasmid[45] were grown and diluted to an A^{600nm}–0.08, suspended in LB-media containing ampicillin (30 μg ml^{-1}) with 15% v/v of Percoll and loaded into a syringe (Hamilton, Gastight, 250 μl), the second identical syringe containing LB-media with various concentrations of OdDHL. Cells were injected into the microfluidic device in 1 : 1 volume ratio with OdDHL solutions and emulsified with fluorinated oil (FC-40, Fluorinert™) mixed with EA-surfactant in a flow focusing device (Fig. S1a†).

Results and discussion

Protein crystallization

Protein crystallization is an activated process due to the energy barrier that prevents crystals below a certain size from growing.[46] To grow crystals effectively, it is necessary for protein solutions to initially be highly supersaturated leading to the formation of many small crystal nuclei that subsequently grow into large crystals at lower levels of supersaturation.

In this study a highly supersaturated solution of lysozyme was achieved by supplying ethanol *via* the reservoir to droplets

containing proteins stored in the wells in the microfluidic device. Fig. 1b–e shows the process of crystal growth in microdroplets. Initially droplets contained a high concentration of lysozyme, approximately equivalent to the maximal solubility in water (59 mg ml^{-1} in 0.2 M sodium chloride, 0.05 M sodium acetate, pH 4.5) (Fig. 1b and S2a†). When neat ethanol was supplied *via* the reservoir channels, the permeability of PDMS[28] resulted in an increase of the ethanol content in the droplet. The solubility of lysozyme in ethanol is about 300-fold lower (0.2 mg ml^{-1})[47] than it is in aqueous solution,[48] so the addition of ethanol reduced the solubility of the protein and created a supersaturated solution, at which point the protein precipitated in minutes (Fig. 1c and S2b†). Such precipitation is frequently observed in highly supersaturated protein solutions, which is in non-equilibrium state, and is thought to provide seeds for crystallization.[37,49]

Although supersaturation is required to nucleate seed crystals, a subsequent lower degree of supersaturation is necessary for crystal growth.[50] In the next step for protein crystallization, the reservoir content was changed to water. The ethanol in the droplets was exchanged *via* the PDMS for the water supplied from the reservoir channel, thus lowering the ethanol content in droplets and dissolving the precipitate over a period of hours (Fig. 1d and S2c†) to allow crystal growth thereafter. The images shown in Fig. 1 illustrate this process of transforming many small crystals into fewer, but larger, crystals over 39 hours (Fig. 1e).[51]

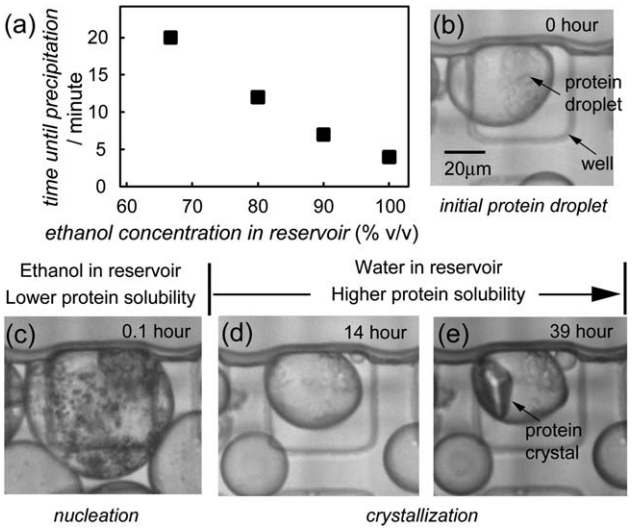

Fig. 1 (a) The time until the precipitation of protein depends on the concentration of ethanol introduced into the reservoir. The plot shows the time until protein precipitation could be observed in droplets as a function of the ethanol content in the reservoir channel. (b) A stable protein solution of lysozyme stored in wells at the beginning of the experiment. (c) Precipitation occurred 6 minutes after the reservoir was filled with 100% ethanol. Ethanol transported from the reservoir to the droplets, increasing ethanol contents in droplets thereby lowering the protein solubility. (d and e) After the reservoir channel was filled with pure water, ethanol continued to evaporate from droplets and was replaced with water. This increased the solubility of the protein in the microdroplets and the precipitate dissolved (d) and crystals were subsequently formed over 39 hours (e). The size of protein crystals in droplets varied between 5–30 μm diameter. A time lapse movie shows this process (see the ESI†).

Some conventional crystallization approaches rely on irreversible kinetic processes to partially decouple crystal nucleation and growth,[52] which are difficult to control and optimize. Microdialysis methods permit independent control of nucleation and growth[53] and this has been implemented in microfluidics.[37,54] Our experiments show that protein crystal nucleation and growth can be independently manipulated by reversibly controlling the protein solubility in microdroplets.

In order to further demonstrate the control of ethanol content in droplets, various concentrations of ethanol were introduced into the reservoir channel and the time until protein precipitation was measured. For example, precipitation took 20 minutes in 66.7% v/v ethanol in the reservoir channel, but using 100% ethanol in the reservoir channel decreased the precipitation time to only 4 minutes (Fig. 1a). As the diffusion coefficient of ethanol[55] in PDMS is 1.7 $\mu m^2 s^{-1}$ and the membrane thickness is about 15 μm (Fig. S1b, ESI†), we estimate that it takes ~2 minutes for ethanol to cross the PDMS membrane based on the diffusion equation, $t = d^2/D$, where t is the time, d the membrane thickness and D the diffusion coefficient. Therefore, the difference in time until precipitation as a function of the ethanol concentrations can be ascribed to differences in the ethanol flux crossing the PDMS membrane from reservoir to droplets since higher concentrations in the reservoir would enhance the ethanol sorption into the PDMS. It should be noted that ethanol-induced swelling of the PDMS would reduce the heights of the channels and this distorted the shape and diameter of the droplets, making it impossible to quantify the ethanol concentration in the droplets (Fig. 1c and S2b†). No protein precipitation was observed when concentrations of ethanol in the reservoir were lower than 50% v/v.

Monitoring activation of gene expression by 3-(oxododecanoyl)-L-homoserine lactone (OdDHL)

The observed permeability of PDMS to ethanol prompted us to investigate whether small organic signaling molecules might be delivered to cells entrapped in microdroplets. We used the ability of cells to respond to auto-inducers (AI) during quorum sensing (QS). Over the last decade, many species of bacteria have been shown to respond to self-produced QS signals.[56–60]

In contrast to QS *in vivo*, which responds to endogenously produced AI, in this work the signaling molecule was supplied exogenously and detected using a genetically reconstituted version of the *las* QS system of *Pseudomonas aeruginosa* (expressed in a heterologous host, *E. coli*).[45,58,61] Here, exogenously supplied *N*-(3-oxododecanoyl)-L-homoserine lactone (OdDHL) was sensed by plasmid-borne LasR, which subsequently activated the expression of green fluorescent protein (GFP) (Fig. 2a).

Fig. 2c shows GFP production in encapsulated cells triggered by the presence of OdDHL (10 μM) in the reservoir channels, suggesting OdDHL diffused readily through the PDMS membrane. In contrast, in the absence of an external trigger, cells did not produce GFP, showing that the plasmid-based reporter system used is sufficiently tightly controlled to yield no appreciable GFP expression under these conditions (Fig. S3†).

The total production of GFP in each droplet varied considerably, giving rise to a 20-fold difference in measured

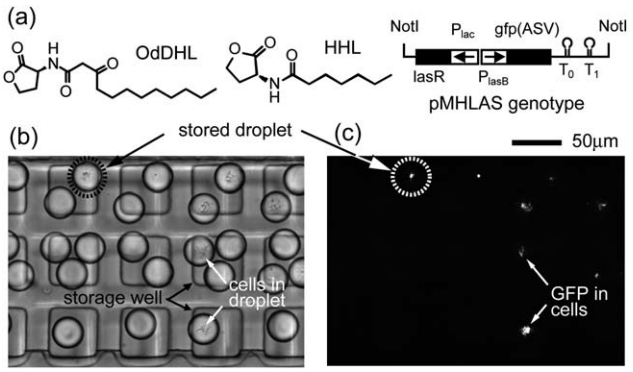

Fig. 2 (a) The chemical structure of OdDHL (*N*-(3-oxododecanoyl)-L-homoserine lactone), HHL (*N*-heptanoyl-L-homoserine lactone) and the insert in the pMHLAS plasmid encoding the LasR dependent QS reporter gene.[46] (b) A bright-field image of droplets stored in square wells. The small spots seen in some microdroplets are the fraction of cells that are in focus. (c) Fluorescence image showing GFP expression at 10 hours after droplet formation in the presence of 10 μM OdDHL in the reservoir. The bright spots are cells expressing GFP while encapsulated in microdroplets.

fluorescence values around an average of 1.3×10^4 RFU after 12 hours (Fig. 3a). The significant differences in GFP production between droplets can be ascribed to different initial cell occupancies in droplets as a consequence of Poissonian encapsulation of cells[8] and the variation in expression levels in individual cells at a given concentration of auto-inducer.[7,9] The latter may be related to variations in the plasmid copy number in each cell as well as cell division on the timescale of the experiment.

Concentration dependence of OdDHL delivery

We next examined the OdDHL concentration dependence of GFP expression in this system. GFP fluorescence was measured from droplets encapsulating cells in which a range of concentrations of OdDHL had been added at the time of droplet formation (Fig. 3c). The time course of GFP expression showed the onset to be around one hour after droplet formation. The lag time between droplet formation and observation of GFP suggests that time was required for the synthesis and maturation of the protein fluorophore.[62] Fig. 3b shows GFP production as a function of OdDHL concentration introduced in the reservoir. When OdDHL was delivered through PDMS, the onset of GFP fluorescence was delayed slightly more, presumably reflecting the time required for the OdDHL to diffuse across the membrane and to accumulate in the droplets. In both cases, GFP production increased over the next few hours and displayed saturation, especially at the higher concentrations of OdDHL tested.[63] The magnitude of the GFP signal was strongly dependent on the OdDHL concentration but reached a maximum when the concentration was above 0.1 μM (Fig. 4a). Notably, the average signal intensity at the saturation point was comparable, irrespective of the method used to deliver the OdDHL.

As shown in Fig. 4a and b, very few cells produced GFP in the presence of 0.01 μM of OdDHL; the amount of GFP produced was 25-fold less than that generated in the presence of 100 μM OdDHL co-encapsulated with an identical cell preparation. The amount of GFP increased to a maximum around 1.35×10^4 RFU at concentrations over 0.1 μM OdDHL. While the final averaged amount of GFP was independent of the delivery method employed, the fraction of droplets producing GFP differed. When OdDHL was directly mixed with cells in droplets the fraction of droplets producing GFP started to increase at 0.01 μM (only four out of 959 droplets) and saturated around 1 μM (approximately 80% of cell-containing droplets) (squares in Fig. 4b). By contrast, when the auto-inducer was delivered through the PDMS membrane, the fraction of droplets producing GFP slowly started to increase from 0.5% at 0.1 μM to 60% when saturation was reached at 100 μM (circles in Fig. 4b). This difference can be ascribed to differences in the actual amount of OdDHL available to cells due to the slow diffusion of OdDHL from reservoir to droplet, thus limiting GFP expression. The difference in the fraction of cells expressing GFP (dashed lines in Fig. 4b) suggests that only ~1% of the OdDHL introduced in the reservoir is delivered into the droplet through the membrane.

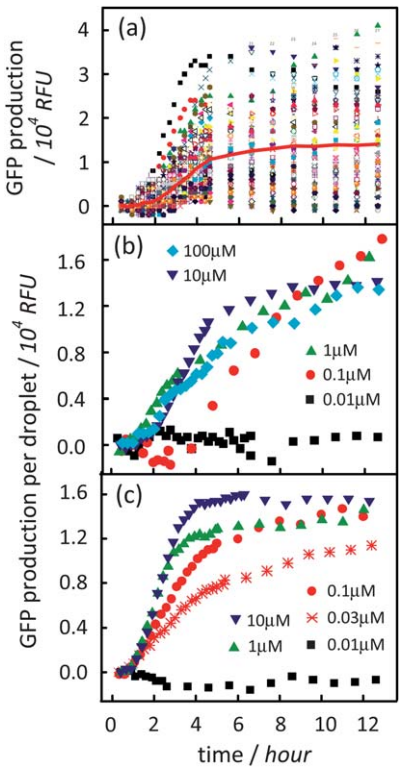

Fig. 3 (a) Kinetics of GFP production by *E. coli* cells encapsulated in microdroplets in the presence of 10 μM OdDHL in the reservoir. The graph shows time traces of fluorescence, which were measured at every 20 minutes up to 5 hours and every hour afterwards; the solid line represents the average. Each symbol corresponds to a droplet containing cells. In these data, 105 droplets out of 620 showed GFP expression and were included in the analysis. (b and c) Time course of GFP expression per droplet at different OdDHL concentrations. OdDHL supplied (b) *via* the reservoir or (c) at the time of droplet formation. The dependence of OdDHL concentrations is similar to experiments using plate reader detection (Fig. S4†).

The reservoir channels constructed under the wells allow the sequential addition of different molecules to droplets. This can be used to modulate cellular responses. The initial droplet and reservoir contents were 100 nM OdDHL and water, respectively. Around 3.5 hours after droplet formation, the reservoir content

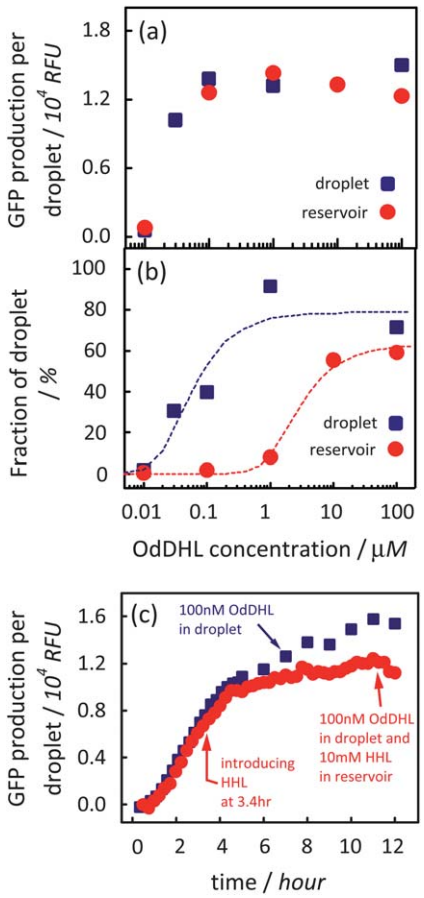

Fig. 4 (a) GFP production per droplet at 12 hours after droplet formation as a function of OdDHL concentration and delivery methods, squares representing direct mixing in the droplets and circles delivery *via* the reservoir. (b) Droplet fractions able to produce GFP at given OdDHL concentrations. In all plots, more than 500 droplets were monitored to calculate the average numbers shown. The dashed lines are for guiding eyes. (c) Kinetics of GFP production in controlled microenvironments. The square represents the experiment in the presence of 100 nM OdDHL in microdroplets and water in reservoir for 13 hours, which is an average of 87 droplets out of 670. The circle shows GFP production in varied microenvironments (an average from 153 droplets). The experimental condition was initially 100 nM OdDHL in droplets and water in reservoir. At 3.5 hours after the droplet formation, the reservoir content was replaced with 10 mM HHL.

was changed to 10 mM *N*-heptanoyl-L-homoserine lactone (HHL) instead of pure water (circle in Fig. 4c). HHL is a quorum sensing molecule involved in the RaiI/RaiR circuit in *Rhizobium leguminosarum*.[64,65] Shorter chain homoserine lactones such as HHL are very weak activators of LasR that compete with OdDHL and inhibit QS.[66–68]

Although the bacteria were already 'switched on' by OdDHL that was co-compartmentalized during droplet formation, the introduction of HHL to the reservoir resulted in a slow down in GFP production after about 5 hours (Fig. 4c). This suggests that HHL was delivered to stored droplets from the reservoir and antagonized the action of OdDHL. The delay between the introduction of HHL and the cellular responses is presumably due to the slow diffusion process of molecules across the membrane, which is consistent with the delay time observed in Fig. 3b.

Conclusions

We have shown, using two very different experimental systems, that delivery of small molecules through PDMS membranes allows the contents of stored droplets in a microfluidic device to be manipulated. Small molecules delivered to droplets were shown to trigger processes as diverse as protein crystallization or quorum sensing in bacteria.

This approach does not require additional device features for droplet fusion such as synchronized lasers or electrodes.[66] Furthermore, the delivery through PDMS is open to all molecules that are soluble in PDMS. The broad correlation of calculated log *P* values and the solubility parameter (Fig. S5†) can be used to estimate their permeability. A drawback of this approach is that it is difficult to estimate the concentration of small molecule that diffuses through the PDMS. This is further compounded because the ethanol swells the PDMS to make the channel height unpredictable and the observables in these experiments were not linearly proportional to the amount of compound accumulated in droplets. It may be possible to get some estimate of the concentration of solutes delivered to droplets by measuring the permeability of fluorescent dye in PDMS, which has a similar log *P* value to OdDHL or HHL. Despite this limitation, the approach clearly has applications in areas where a threshold concentration is required to trigger a process or where longer term change in a droplet content is required.

Acknowledgements

This work was supported by the RCUK Basic Technology Programme and an EPSRC platform grant. JUS holds an EU Marie-Curie fellowship. FH is an ERC Starting Investigator. We also thank the BBSRC, MRC and Frances and Augustus Newman Foundation for financial support.

References

1 A. Huebner, S. Sharma, M. Srisa-Art, F. Hollfelder, J. B. Edel and A. J. Demello, *Lab Chip*, 2008, **8**, 1244–1254.
2 Y. Schaerli and F. Hollfelder, *Mol. BioSyst.*, 2009, **5**, 1392–1404.
3 S. Y. Teh, R. Lin, L. H. Hung and A. P. Lee, *Lab Chip*, 2008, **8**, 198–220.
4 A. B. Theberge, F. Courtois, Y. Schaerli, M. Fischlechner, C. Abell, F. Hollfelder and W. T. S. Huck, *Angew. Chem., Int. Ed.*, 2010, **49**, 5846–5868.
5 B. Kintses, L. van Vliet, S. Devenish and F. Hollfelder, *Curr. Opin. Chem. Biol.*, 2010, **15**, 548–555.
6 C. N. Baroud, F. Gallaire and R. Dangla, *Lab Chip*, 2010, **10**, 2032–2045.
7 C. H. J. Schmitz, A. C. Rowat, S. Koster and D. A. Weitz, *Lab Chip*, 2009, **9**, 44–49.
8 J. Clausell-Tormos, D. Lieber, J. C. Baret, A. El-Harrak, O. J. Miller, L. Frenz, J. Blouwolff, K. J. Humphry, S. Koster, H. Duan, C. Holtze, D. A. Weitz, A. D. Griffiths and C. A. Merten, *Chem. Biol.*, 2008, **15**, 427–437.
9 J. U. Shim, L. F. Olguin, G. Whyte, D. Scott, A. Babtie, C. Abell, W. T. S. Huck and F. Hollfelder, *J. Am. Chem. Soc.*, 2009, **131**, 15251–15256.
10 J. Tang, A. M. Jofre, G. M. Lowman, R. B. Kishore, J. E. Reiner, K. Helmerson, L. S. Goldner and M. E. Greene, *Langmuir*, 2008, **24**, 4975–4978.
11 F. Courtois, L. F. Olguin, G. Whyte, A. B. Theberge, W. T. S. Huck, F. Hollfelder and C. Abell, *Anal. Chem.*, 2009, **81**, 3008–3016.
12 M. Kumemura and T. Korenaga, *Anal. Chim. Acta*, 2006, **558**, 75–79.

13 P. Mary, V. Studer and P. Tabeling, *Anal. Chem.*, 2008, **80**, 2680–2687.
14 C. Holtze, A. C. Rowat, J. J. Agresti, J. B. Hutchison, F. E. Angile, C. H. J. Schmitz, S. Koster, H. Duan, K. J. Humphry, R. A. Scanga, J. S. Johnson, D. Pisignano and D. A. Weitz, *Lab Chip*, 2008, **8**, 1632–1639.
15 L. S. Roach, H. Song and R. F. Ismagilov, *Anal. Chem.*, 2005, **77**, 785–796.
16 D. J. Holt, R. J. Payne and C. Abell, *J. Fluorine Chem.*, 2010, **131**, 398–407.
17 K. Ahn, J. Agresti, H. Chong, M. Marquez and D. A. Weitz, *Appl. Phys. Lett.*, 2006, **88**, 264105.
18 D. R. Link, E. Grasland-Mongrain, A. Duri, F. Sarrazin, Z. D. Cheng, G. Cristobal, M. Marquez and D. A. Weitz, *Angew. Chem., Int. Ed.*, 2006, **45**, 2556–2560.
19 X. Z. Niu, F. Gielen, A. J. deMello and J. B. Edel, *Anal. Chem.*, 2009, **81**, 7321–7325.
20 A. R. Abate, T. Hung, P. Mary, J. J. Agresti and D. A. Weitz, *Proc. Natl. Acad. Sci. U. S. A.*, 2010, **107**, 19163–19166.
21 L. Mazutis, A. F. Araghi, O. J. Miller, J. C. Baret, L. Frenz, A. Janoshazi, V. Taly, B. J. Miller, J. B. Hutchison, D. Link, A. D. Griffiths and M. Ryckelynck, *Anal. Chem.*, 2009, **81**, 4813–4821.
22 E. Um and J. K. Park, *Lab Chip*, 2009, **9**, 207–212.
23 C. J. Gerdts, V. Tereshko, M. K. Yadav, I. Dementieva, F. Collart, A. Joachimiak, R. C. Stevens, P. Kuhn, A. Kossiakoff and R. F. Ismagilov, *Angew. Chem., Int. Ed.*, 2006, **45**, 8156–8160.
24 L. M. Fidalgo, C. Abell and W. T. S. Huck, *Lab Chip*, 2007, **7**, 984–986.
25 C. Priest, S. Herminghaus and R. Seemann, *Appl. Phys. Lett.*, 2006, **88**, 3.
26 C. N. Baroud, M. R. de Saint Vincent and J. P. Delville, *Lab Chip*, 2007, **7**, 1029–1033.
27 E. Verneuil, M. Cordero, F. Gallaire and C. N. Baroud, *Langmuir*, 2009, **25**, 5127–5134.
28 J. N. Lee, C. Park and G. M. Whitesides, *Anal. Chem.*, 2003, **75**, 6544–6554.
29 M. W. Toepke and D. J. Beebe, *Lab Chip*, 2006, **6**, 1484–1486.
30 E. Baltussen, F. David, P. Sandra, H. G. Janssen and C. Cramers, *J. Microcolumn Sep.*, 1999, **11**, 471–474.
31 T. Mohammadi, A. Aroujalian and A. Bakhshi, *Chem. Eng. Sci.*, 2005, **60**, 1875–1880.
32 E. Ostuni, C. S. Chen, D. E. Ingber and G. M. Whitesides, *Langmuir*, 2001, **17**, 2828–2834.
33 S. Jon, J. Seong, A. Khademhosseini, T.-N. T. Tran, P. E. Laibinis and R. Langer, *Langmuir*, 2003, **19**, 9989–9993.
34 W. J. Chang, D. Akin, M. Sedlak, M. R. Ladisch and R. Bashir, *Biomed. Microdevices*, 2003, **5**, 281–290.
35 K. J. Regehr, M. Domenech, J. T. Koepsel, K. C. Carver, S. J. Ellison-Zelski, W. L. Murphy, L. A. Schuler, E. T. Alarid and D. J. Beebe, *Lab Chip*, 2009, **9**, 2132–2139.
36 M. A. Unger, H. P. Chou, T. Thorsen, A. Scherer and S. R. Quake, *Science*, 2000, **288**, 113–116.
37 J. U. Shim, G. Cristobal, D. R. Link, T. Thorsen, Y. W. Jia, K. Piattelli and S. Fraden, *J. Am. Chem.Soc.*, 2007, **129**, 8825–8835.
38 B. Zheng, L. S. Roach and R. F. Ismagilov, *J. Am. Chem. Soc.*, 2003, **125**, 11170–11171.
39 L. Li and R. F. Ismagilov, *Annu. Rev. Biophys.*, 2010, **39**, 139–158.
40 J. Q. Boedicker, M. E. Vincent and R. F. Ismagilov, *Angew. Chem., Int. Ed.*, 2009, **48**, 5908–5911.
41 E. C. Carnes, D. M. Lopez, N. P. Donegan, A. Cheung, H. Gresham, G. S. Timmins and C. J. Brinker, *Nat. Chem. Biol.*, 2010, **6**, 41–45.
42 V. Studer, G. Hang, A. Pandolfi, M. Ortiz, W. F. Anderson and S. R. Quake, *J. Appl. Phys.*, 2004, **95**, 393–398.
43 W. Schrott, M. Svoboda, Z. Slouka, M. Pribyl and D. Snita, *Microelectron. Eng.*, 2010, **87**, 1600–1602.
44 D. C. Duffy, J. C. McDonald, O. J. A. Schueller and G. M. Whitesides, *Anal. Chem.*, 1998, **70**, 4974–4984.
45 M. Hentzer, K. Riedel, T. B. Rasmussen, A. Heydorn, J. B. Andersen, M. R. Parsek, S. A. Rice, L. Eberl, S. Molin, N. Hoiby, S. Kjelleberg and M. Givskov, *Microbiology*, 2002, **148**, 87–102.
46 J. M. Garcia-Ruiz, *J. Struct. Biol.*, 2003, **142**, 22–31.
47 L. E. Bromberg and A. M. Klibanov, *Proc. Natl. Acad. Sci. U. S. A.*, 1995, **92**, 1262–1266.
48 I. Broutin, M. Rieskautt and A. Ducruix, *J. Appl. Crystallogr.*, 1995, **28**, 614–617.
49 M. Muschol and F. Rosenberger, *J. Chem. Phys.*, 1997, **107**, 1953–1962.
50 A. McPherson, *Crystallization of Biological Macromolecules*, Cold Spring Harbor Laboratory Press, Cold Spring Harbor, NY, 1999.
51 P. G. Debenedetti, *Metastable Liquids: Concepts and Principles*, Princeton University Press, Princeton, NJ, 1996.
52 N. E. Chayen, *Prog. Biophys. Mol. Biol.*, 2005, **88**, 329–337.
53 H. W. Smith and L. J. Delucas, *J. Cryst. Growth*, 1991, **110**, 137–141.
54 J. U. Shim, G. Cristobal, D. R. Link, T. Thorsen and S. Fraden, *Cryst. Growth Des.*, 2007, **7**, 2192–2194.
55 Y. M. Lee, D. Bourgeois and G. Belfort, *J. Membr. Sci.*, 1989, **44**, 161–181.
56 M. B. Miller and B. L. Bassler, *Annu. Rev. Microbiol.*, 2001, **55**, 165–199.
57 D. Smith, J.-H. Wang, J. E. Swatton, P. Davenport, B. Price, H. Mikkelsen, H. Stickland, K. Nishikawa, N. Gardiol, D. R. Spring and M. Welch, *Sci. Prog.*, 2006, **89**, 167–211.
58 V. E. Wagner and B. H. Iglewski, *Clin. Rev. Allergy Immunol.*, 2008, **35**, 124–134.
59 C. M. Waters and B. L. Bassler, *Annu. Rev. Cell Dev. Biol.*, 2005, **21**, 319–346.
60 M. Welch, H. Mikkelsen, J. E. Swatton, D. Smith, G. L. Thomas, F. G. Glansdorp and D. R. Spring, *Mol. BioSyst.*, 2005, **1**, 196–202.
61 J. W. Costerton, P. S. Stewart and E. P. Greenberg, *Science*, 1999, **284**, 1318–1322.
62 J. B. Andersen, A. Heydorn, M. Hentzer, L. Eberl, O. Geisenberger, B. B. Christensen, S. Molin and M. Givskov, *Appl. Environ. Microbiol.*, 2001, **67**, 575–585.
63 A. Ishihama, *Genes Cells*, 1999, **4**, 135–143.
64 A. M. L. Barnard and G. P. C. Salmond, *Complexus*, 2005, **2**, 87–101.
65 J. K. Lithgow, A. Wilkinson, A. Hardman, B. Rodelas, F. Wisniewski-Dye, P. Williams and J. A. Downie, *Mol. Microbiol.*, 2000, **37**, 81–97.
66 K. Churski, P. Korczyk and P. Garstecki, *Lab Chip*, 2010, **10**, 816–818.
67 M. E. Mattmann and H. E. Blackwell, *J. Org. Chem.*, 2010, **75**, 6737–6746.
68 M. K. Winson, S. Swift, P. J. Hill, C. M. Sims, G. Griesmayr, B. W. Bycroft, P. Williams and G. Stewart, *FEMS Microbiol. Lett.*, 1998, **163**, 193–202.